NASA TECHNICAL NOTE

NASA TN D-2621

NASA TN D-2621

OFF-DESIGN PERFORMANCE PREDICTION WITH EXPERIMENTAL VERIFICATION FOR A RADIAL-INFLOW TURBINE

by Samuel M. Futral, Jr., and Charles A. Wasserbauer

Lewis Research Center

Cleveland, Ohio

NATIONAL AERONAUTICS AND SPACE ADMINISTRATION • WASHINGTON, D. C. • FEBRUARY 1965

NASA TN D-2621

OFF-DESIGN PERFORMANCE PREDICTION WITH EXPERIMENTAL VERIFICATION FOR A RADIAL-INFLOW TURBINE

By Samuel M. Futral, Jr., and Charles A. Wasserbauer

Lewis Research Center
Cleveland, Ohio

NATIONAL AERONAUTICS AND SPACE ADMINISTRATION

For sale by the Office of Technical Services, Department of Commerce,
Washington, D.C. 20230 -- Price $2.00

OFF-DESIGN PERFORMANCE PREDICTION WITH EXPERIMENTAL VERIFICATION FOR A RADIAL-INFLOW TURBINE

by Samuel M. Futral, Jr., and Charles A. Wasserbauer

Lewis Research Center

SUMMARY

A method for predicting the off-design performance of a radial-inflow gas turbine is presented. The equations used have been programed for a digital computer. Input to the program must include the turbine geometry and dimensions. The efficiency, pressure ratio, speed, and weight flow at a given operating point are necessary in order to evaluate the loss coefficients.

Predicted performance is given for a 4.5-inch-diameter commercial turbine. Comparison of predicted with experimentally determined performance for this turbine showed good agreement.

Radial turbine performance differs from that of the axial turbine because of centrifugal forces set up by the radius change. Thus, weight-flow and, consequently, stator-flow conditions and rotor incidence loss are more sensitive to speed than in axial machines. The operating range is therefore limited by the centrifugal forces that cause flow and specific work to become negative at blade-jet speed ratios near 1.0.

INTRODUCTION

Space power systems for the generation of power in the 10-kilowatt range are currently under study within NASA. At such low power levels, the efficiency of axial-flow turbines is reduced, since clearances become more significant compared with blade height as size decreases. In addition, there is difficulty in maintaining the proper tolerances in the blade profiles. The fact that the efficiency of the radial-inflow turbine is relatively insensitive to these effects as the size decreases has resulted in an advantage for the radial-inflow turbine in the smaller sizes.

Discussions of closed gas systems for power generation in space, which may utilize radial-inflow turbines, are given in references 1 and 2. A broad discussion of the capabilities of radial-inflow turbines, operating at design con-

ditions, is given in reference 3; however, a method is needed for predicting off-design performance for use in systems where there are variations in such quantities as wheel speed, load, and pressure ratio.

A procedure for predicting off-design performance for axial-flow turbines has been presented in reference 4. Essentially the same procedure was used herein; however, it was necessary to take into account certain differences between these two types of turbines. The principal difference is that a radius change occurs within the rotor of the radial-inflow turbine. This results in a change in the total temperature, relative to the rotor, between rotor inlet and rotor exit. The other difference between axial-flow and radial-inflow turbines, which made different analytical procedures necessary, was the radial clearance between the stator exit and rotor inlet.

The task of producing the necessary set of equations, suitable for use with a high-speed digital computer, was undertaken at Lewis Research Center. In order to use the method, the efficiency, speed, weight flow rate, and overall pressure ratio must be known or estimated at an important operating point, such as the design point. This information is used to evaluate the loss coefficients.

The method for predicting the off-design performance is presented in this report. Performance prediction is made for a commercial turbine of 4.5-inch rotor-tip diameter. Results of the prediction are compared with the performance determined experimentally at Lewis.

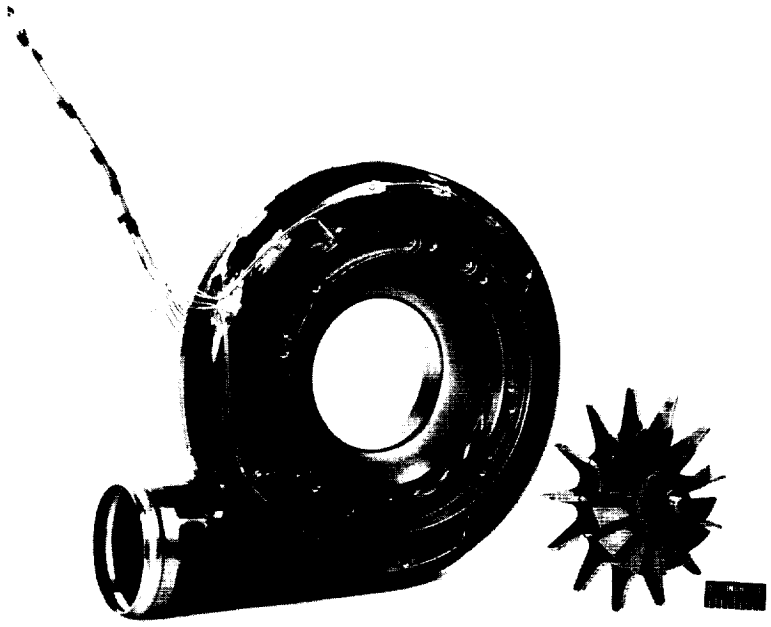

C-72088

Figure 1. - Turbine stator-scroll component and rotor.

DESCRIPTION OF TURBINE MODEL

A single-stage 4.5-inch-diameter commercial radial-inflow turbine was used as a model for the analysis. The stator and rotor of this turbine are shown in figure 1, and the axial and radial cross sections through the turbine with station designation are shown in figure 2. The turbine has 13 blades and normally uses air as a working fluid at the following operating conditions:

Inlet total pressure, p_0', lb/sq ft	6652.8
Inlet total temperature, T_0', $^\circ R$	592.0
Rotational speed, rpm	51 500.0
Ratio of inlet total to exit total pressure, p_0'/p_4'	3.0

All symbols are defined in appendix A.

Certain reference conditions needed in the analysis were determined from experimental measurements and are given as follows:

Equivalent weight flow, $(w\sqrt{\theta_{cr}})/\delta$, lb/sec	0.3455
Ratio of inlet total to exit static pressure, p_0'/p_4	3.25
Static efficiency, η_s	0.756
Equivalent speed, rpm	48 205.0

In addition to the operating and reference conditions, various turbine physical characteristics were also needed. These values were measured directly from the turbine:

Area of turbine inlet, A_0, sq ft	0.04231
Area at station immediately upstream of stator exit, A_1, sq ft	.01773
Area at station immediately upstream of rotor inlet, A_3, sq ft	.03112
Area at station immediately downstream of rotor exit, A_4, sq ft	.03850
Radius at station immediately upstream of stator exit, r_1, in.	2.45
Radius at station immediately upstream of rotor inlet, r_3, in.	2.25
Radius at station immediately downstream of rotor exit, r_4, in.	1.15
Absolute gas angle, α, deg	63.75

All areas given are normal to the meridional velocity component, which is the velocity component lying in a plane containing the axis of rotation. The radius at station 4 divides the exit annulus into equal areas and was so selected because of the low hub-tip radius ratio of 0.46. The study in reference 4 of an axial turbine used the arithmetic mean of the hub and tip radii. The rotor exit angle β_4 is the free-stream gas flow angle at this radius.

A feature of this turbine that had to be taken into account in the analysis was the use of circular nozzles rather than vanes in the stator (see figs. 1 and 2.) There are 23 holes, 0.25 inch in diameter, equally spaced circumferentially around the rotor inlet. This resulted in a 91.2-percent increase in the flow area from just inside the stator exit A_1 to just outside it in the free stream. A radial distance of 0.20 inch separates the stator exit from the rotor inlet.

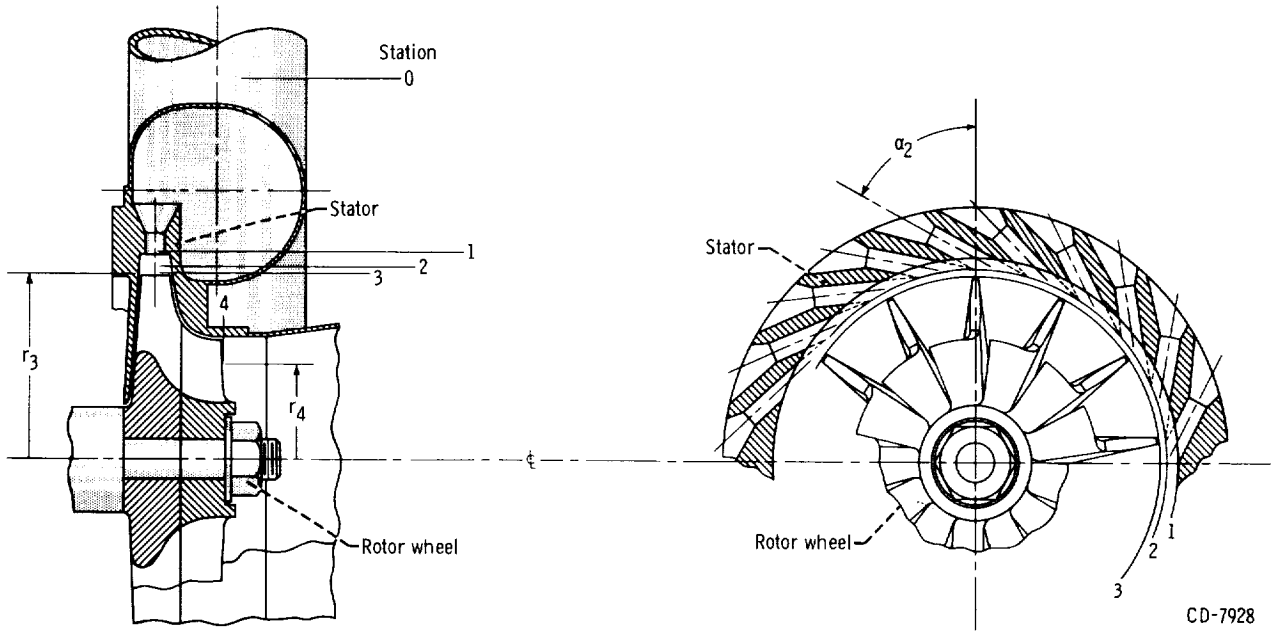

Figure 2. - Diagramatic sketch of turbine stator and rotor.

METHOD OF ANALYSIS

The analysis consists of a step-by-step solution of flow conditions through the turbine along a path approximating the mean streamline in the meridional plane. Perfect gas relations were used throughout. For any fixed speed, the velocity ratio V/V_{cr} at the stator exit is varied by uniform increments, and for each increment, complete calculations are made at each station. The details of these calculations are given in appendix B. The procedure used for writing the equations is essentially the same as that described in reference 4, which deals with axial-flow turbines.

There are three main differences in the analytical procedure. First, the unusual stator configuration, involving large blockage at the stator exit and large radial clearance between the stator and rotor, suggested the use of an additional station, station 2, between the stator and the rotor. This is the station where the flow from the stator is assumed to occupy the entire cylindrical flow area. The location of this station is not constant under all conditions, and its radius must be determined at each operating point.

The second difference arises from the fact that the flow channel experiences a change in radius from the rotor inlet to the rotor exit. This causes a change in the total temperature, relative to the rotor, and results in a modification in the expression for the pressure-loss ratio across the rotor.

The third difference is in the manner of evaluating the viscous loss coefficients. The evaluation of these coefficients is discussed in appendix C, but they will be defined here. The viscous loss in a channel is assumed to be proportional to the average kinetic energy in the channel, where the average kinet-

ic energy is regarded simply as the average of that entering and leaving. This is the same concept as that used in reference 4. The viscous loss between the turbine inlet and the stator exit is given by

$$L_1 = K_1 \frac{V_0^2 + V_1^2}{2gJ} \tag{1}$$

The viscous loss between the turbine inlet and station 2 is given by

$$L_S = K \frac{V_0^2 + V_2^2}{2gJ} \tag{2}$$

The viscous loss in the rotor is given by

$$L_R = mK \frac{W_3^2 + W_4^2}{2gJ} \tag{3}$$

The stator-throat loss coefficient K_1 is different from the overall stator loss coefficient because of the occurrence of additional losses between the throat and station 2. This loss coefficient was determined from data supplied by the manufacturer. The other coefficients, K and m, were selected to make calculated and experimental weight flow and efficiency agree at the reference operating point. Figure 3, a typical set of velocity diagrams, will be helpful in understanding equations (1) to (3).

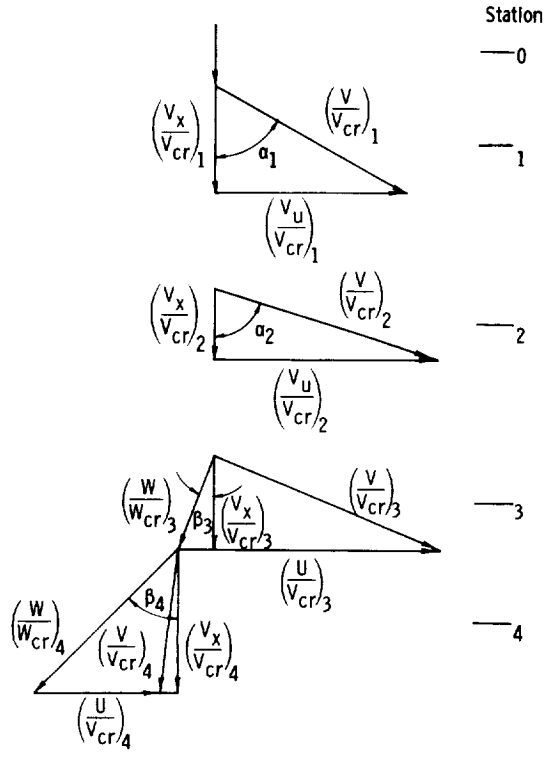

Figure 3. - Turbine velocity diagrams.

For calculating the incidence loss at the rotor inlet, it is assumed, as in the case of axial-flow turbines (ref. 4), that the loss is equivalent to the kinetic energy of the velocity component normal to the blade at the rotor inlet. Additional assumptions have been made in the analysis, namely that the velocity of the flow does not change direction between stations 1 and 2, and the static pressure is constant between these stations, and that the flow is isentropic between stations 2 and 3.

The equations resulting from the analysis are presented in appendix B in the same order in which they were used in the computer program.

APPARATUS, INSTRUMENTATION, AND TEST PROCEDURE

In the experimental investigation, the apparatus consisted of the commercial

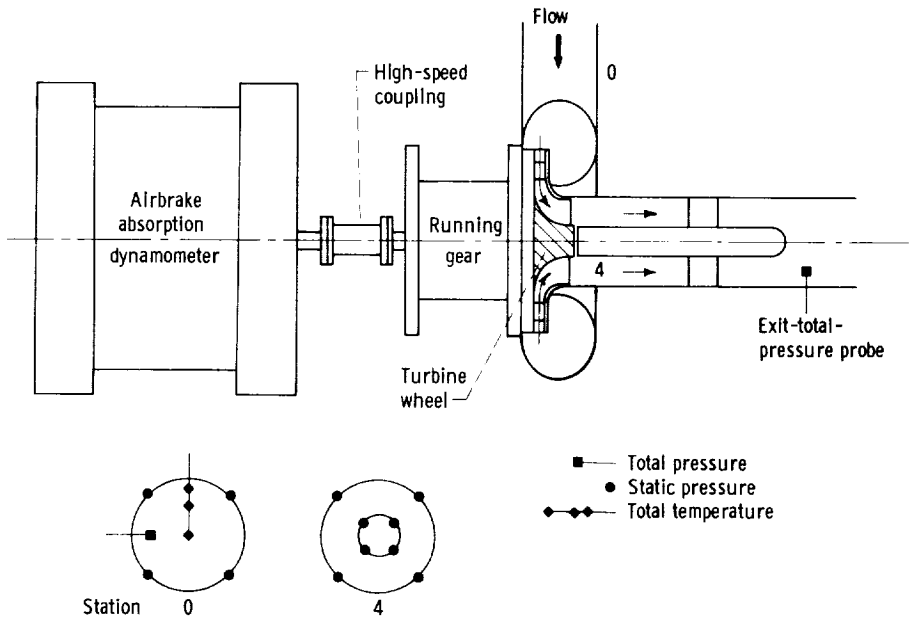

Figure 4. - Sketch of turbine test apparatus.

radial-inflow turbine, a high-speed coupling, and an airbrake absorption dynamometer. A description of the dynamometer and its operation is given in reference 5.

Dry pressurized air from the laboratory combustion air supply was piped to the turbine through a pressure regulator, a sharp-edged orifice run, an emergency shut-off valve, and air filters. Exhaust air was piped into the laboratory exhaust system through various throttle valves. The turbine test apparatus is given in figure 4, and the overall turbine test facility is shown in figure 5.

The weight flow was measured with a sharp-edged orifice that was installed according to the ASME Power Test Code. Turbine-inlet static pressure was obtained from four static taps located at station 0. Another set of four static taps located at both the inner and outer wall at station 4 (see fig. 4) measured the exit static pressure. The inlet total temperature, station 0, was measured with a total-temperature rake consisting of three thermocouples. Two total-pressure probes were also used to set turbine total-pressure ratio. One was located at station 0 and the other at a point approximately 1 foot downstream of the turbine exit; however, the turbine-inlet total pressure used in this report was calculated by using the turbine-inlet static-pressure readings. Figure 4 shows the location of the static- and total-pressure and total-temperature measuring stations.

A six-tooth sprocket mounted on one end of the high-speed coupling was used in conjunction with a magnetic pickup and an electronic tachometer to record speed. A 10-pound commercial strain-gage load cell was used to measure the torque. The turbine was operated at an inlet total pressure of about 28 pounds per square inch absolute with an inlet total temperature of about 83° F. The

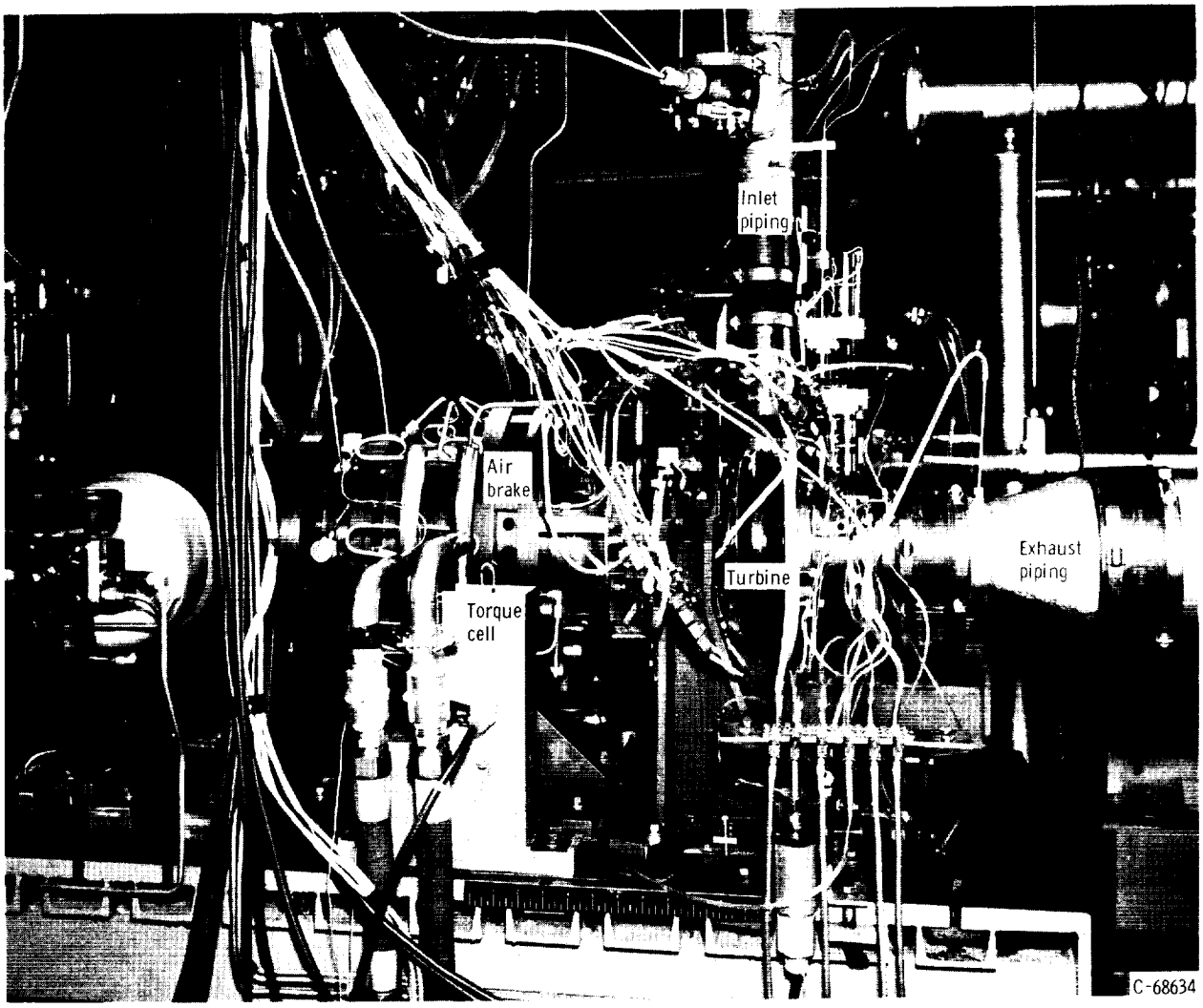

Figure 5. - Installation of turbine test facility.

exit total pressure was varied to obtain a series of pressure ratios from $1\frac{1}{2}$ to 4 across the turbine. At each pressure ratio, turbine speed was varied from 40 to 100 percent of design in 20 percent increments.

In order to obtain turbine friction torque, the air was exhausted from the turbine with the inlet valve closed, and the turbine was driven by the airbrake absorption dynamometer over the entire speed range. The friction torque was measured with a 1-pound commercial strain-gage load cell and was then added to the turbine torque.

RESULTS AND DISCUSSION

Results of the investigation are presented in terms of standard performance parameters to show first the comparison between analytically and experimentally determined performance and second to examine radial turbine operating characteristics.

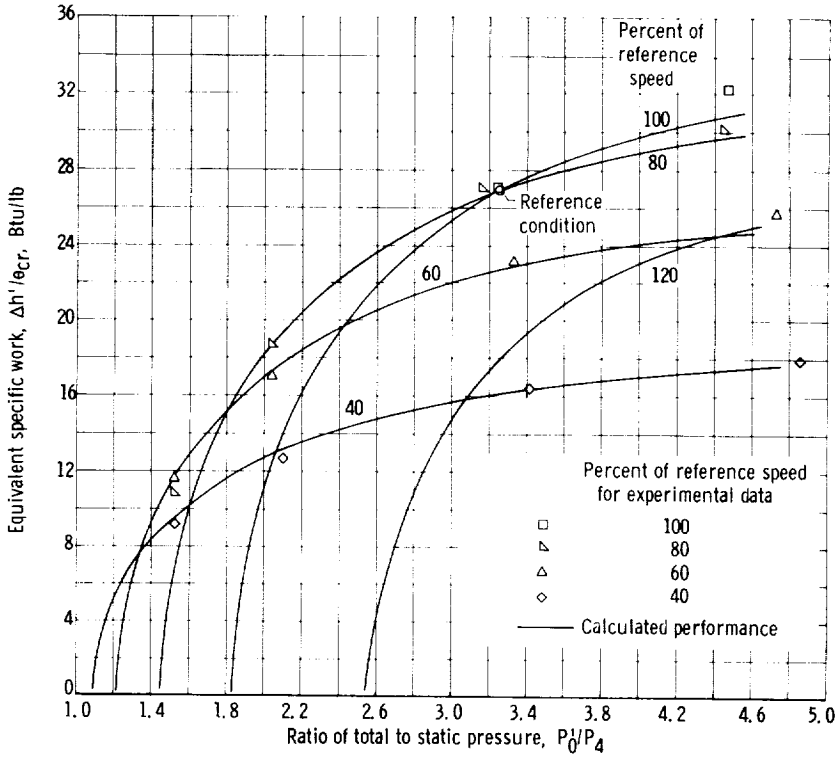

Figure 6. - Variation of equivalent specific work with pressure ratio.

In figure 6 specific work, as calculated, is plotted against total-static pressure ratio for lines of constant speed. The experimental points are also shown for direct comparison. No experimental results are available for 120 percent of reference speed because of limitations of the dynamometer. In taking the experimental data, efforts were made to take data at points of constant speed for a particular run at several fixed pressure ratios. The speed for any experimental point does not differ from that indicated by more than 3.7 percent. Good agreement is shown between the calculated and experimental results.

At the high pressure ratios, figure 6 shows a drop in specific work at 100 and 120 percent of reference speed, with the curve for 120 percent of reference speed being entirely below the curve for 100 percent. This specific-work drop was due to the rotor being choked and resulted in the stator velocities being 19 and 41 percent lower than their choking value at 100 and 120 percent of reference speed, respectively. It may be expected, therefore, that the combination of high wheel speeds and low stator velocities will result in severe incidence losses and a corresponding decrease in work in the high-speed high-pressure-ratio range of operation.

Figure 7 shows the variation in equivalent flow with speed and pressure ratio. The experimental data are in good agreement with the calculated performance at pressure ratios above 3. At pressure ratios below 3, the calculated and experimental performance are in fair agreement where slight changes in pressure ratio have a large effect on weight flow. For example, at a pressure ratio of 1.52 and 80 percent of reference speed, the experimental weight flow is

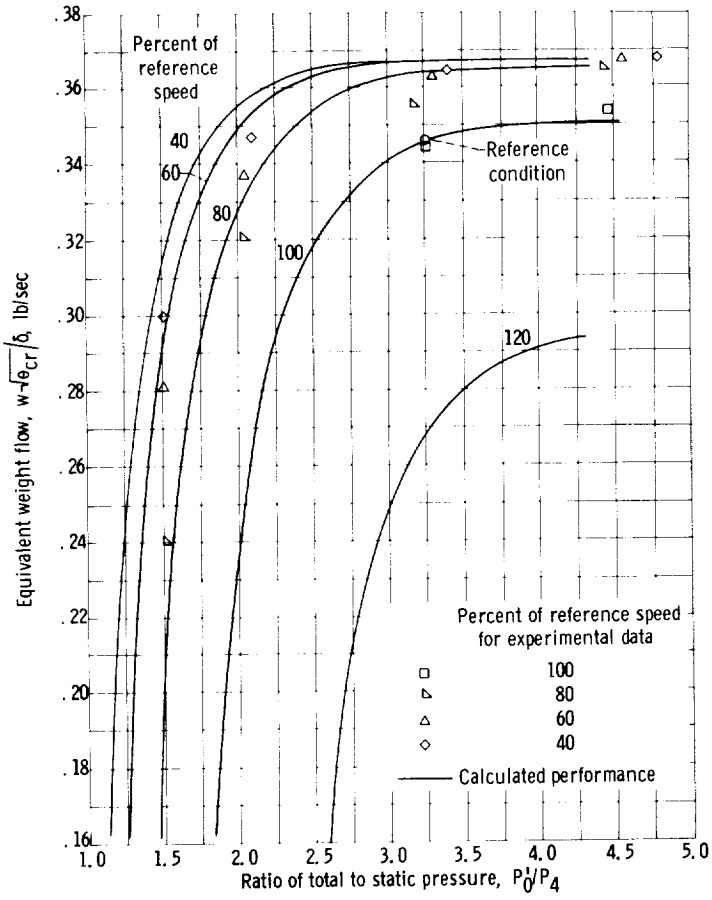

Figure 7. - Variation of equivalent weight flow with pressure ratio.

8.3 percent above the calculated curve. At the same speed and a constant weight flow of 0.24, the difference in pressure ratio is 3 percent.

It may be noted that, at pressure ratios above 3 and speeds below 60 percent of reference, the stator is choked with a limiting flow of 0.367 pound per second. At all other conditions, weight flow decreases rapidly with increasing speed reflecting the centrifugal effects in the turbine rotor. This is perhaps the most significant difference between radial and axial turbines, because, at zero flow, the radial machine shows a pressure ratio greater than 1.

At speeds of 100 and 120 percent of reference speed, the maximum weight flows are appreciably lower than the stator choke flow, 4.4 and 20 percent, respectively. As mentioned previously in the discussion of specific work (fig. 6), the combination of high wheel speeds and low stator velocities results in severe incidence losses. This compounds the effect of speed on weight flow by reducing the rotor-inlet relative total pressure.

The torque-speed relation is shown in figure 8 where the dimensionless torque parameter η_s/ν is plotted against blade-jet speed ratio. The curves shown are results of the performance calculation. The outstanding feature of the torque curves is the deviation from the straight-line characteristic of single-stage axial turbines. This deviation indicates that the radial turbine is less efficient at off-design blade-jet speed ratios than corresponding single-stage axial turbines.

Figure 9 shows the variation in static efficiency with blade-jet speed ratio at speeds of 40, 60, 80, 100, and 120 percent of the reference value. A typical pressure ratio, 2.0, was examined to determine the reason for lower off-design efficiencies than those observed in axial turbines. Calculated losses were compared with the losses presented in reference 6 for a single-stage axial turbine. At low speeds, rotor viscous losses are considerably higher in the radial machine. This may be explained in terms of the radius change in the radial turbine rotor and the centrifugal pressure effect. As speed is decreased, the pressure difference due to rotation decreases, reducing the stator exit

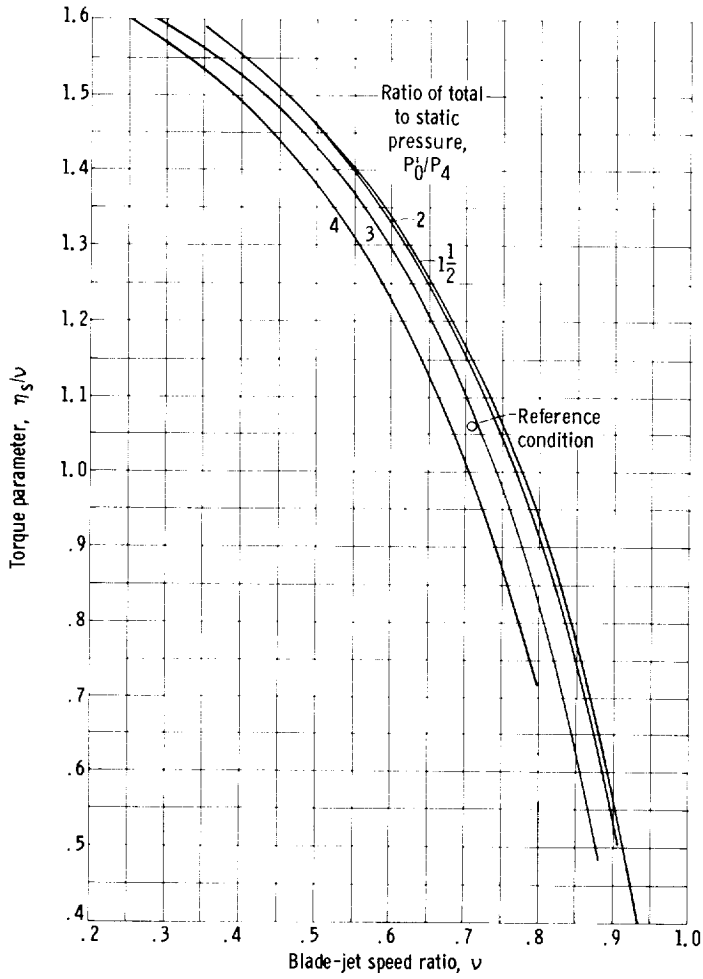

Figure 8. - Calculated torque-speed characteristics.

pressure and therefore increasing flow rate, velocity levels, and viscous losses more rapidly than in the axial turbine. Losses are, therefore, relatively higher in the radial turbine. At high speeds the radial machine shows a far greater increase in incidence loss, indicating again the effect of speed on flow and stator exit velocities. It may be noted here that a fundamental upper limit in attainable blade-jet speed ratio exists in radial turbines. This occurs at blade-jet speed ratios near 1.0, depending on rotor inlet- to outlet-radius ratio, where the turbine pressure ratio corresponds to that of the centrifugal forces generated by rotation. At higher blade-jet speed ratios, flow and specific work go negative and the turbine becomes a compressor.

The high-speed curves for 100 and 120 percent of reference show lower values of peak efficiency as well as an increase in the blade-jet speed ratio at which maximum efficiency occurs. These differences are due to the previously described rotor choking condition that limits stator exit velocities and hence angular momentum available to the rotor. As noted, the stator exit velocity is reduced 41 percent from the choke value at 120 percent of reference speed. The velocity diagrams are therefore altered from the low incidence case at the blade-jet speed ratio near 0.73. Examination of the losses calculated at 120 percent of reference speed indicated that 20 points in efficiency are lost in incidence and that rotor viscous losses have increased from 7 points in efficiency at 80 percent of reference speed to 15 points at 120 percent of reference speed, thus causing the reduction in efficiency at that blade-jet speed ratio. Further examination of the loss calculations showed that the blade-jet speed ratio at which peak efficiency occurs increases because of the relative changes in incidence loss and rotor viscous loss. At constant speed, blade-jet speed ratio increases with decreasing pressure ratio. Rotor viscous losses and leaving losses, therefore, decrease because of decreasing velocity level. In the interval of 0.73 to 0.77 at 120 percent of reference speed, reduction in rotor viscous and leaving losses occurs at a more rapid rate than the increase in incidence loss, resulting in a minimum total loss condition at a blade-jet speed ratio of 0.77.

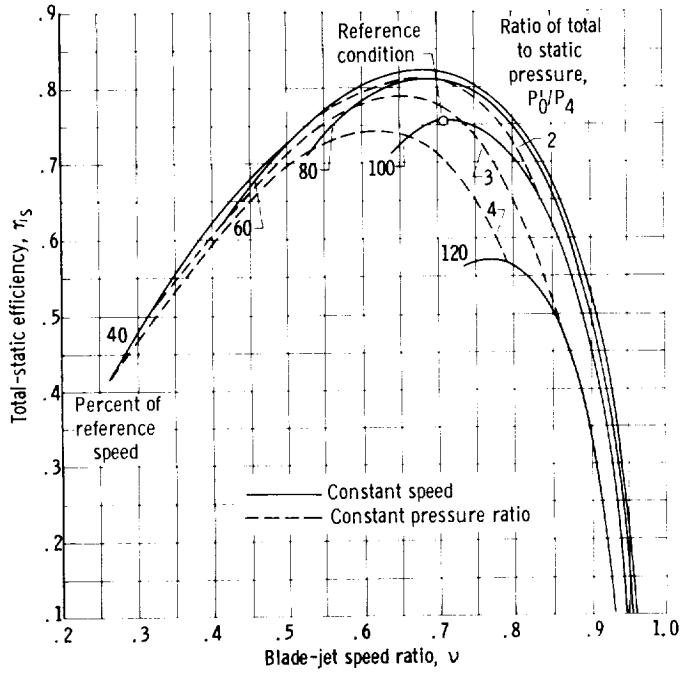

Figure 9. - Calculated turbine efficiency characteristics.

CONCLUSIONS

An analytical method for predicting radial-turbine performance was developed and used to calculate performance characteristics over wide ranges of speed and pressure ratio. Comparison of the calculated results with experimental results obtained for a particular turbine indicates that the method provides good agreement.

Examination of turbine losses for a radial and a single-stage axial turbine showed that the change in radius through the radial turbine was most significant in the centrifugal effect of speed on weight flow.

Lewis Research Center,
National Aeronautics and Space Administration,
Cleveland, Ohio, November 18, 1964.

APPENDIX A

SYMBOLS

A	area, sq ft
c_p	specific heat at constant pressure, Btu/(lb)($^\circ$R)
g	gravitational constant, 32.1741 ft/sec^2
$\Delta h'_{id,s}$	ideal turbine work based on inlet-total- to exit-static-pressure ratio, Btu/lb
$\Delta h'_{id,t}$	ideal turbine work based on inlet-total- to exit-total-pressure ratio, Btu/lb
$\Delta h'$	specific turbine work, Btu/lb
J	mechanical equivalent of heat, 778.029 ft-lb/Btu
K,m	loss coefficients, dimensionless
L	kinetic energy loss, $(V_{id}^2 - V^2)/2gJ$, Btu/lb
l	axial distance, ft
p	pressure, lb/sq ft
r	radius, ft
T	absolute temperature, $^\circ$R
U	blade speed, ft/sec
V	absolute velocity of gas, ft/sec
W	gas velocity relative to rotor, ft/sec
w	weight flow rate, lb/sec
α	absolute gas angle, angle between absolute velocity vector and meridional plane at mean channel, positive when direction of tangential velocity component and direction of wheel velocity agree, and negative when they disagree
β	relative gas angle, angle between the velocity vector relative to wheel and meridional plane at mean channel; same sign convention applies as for α
γ	ratio of specific heat at constant pressure to specific heat at constant volume

δ ratio of turbine-inlet total pressure to U.S. standard atmospheric pressure, $P'_0/2116.22$

η_s efficiency based on ratio of inlet total to exit static pressure

η_t efficiency based on ratio of inlet total to exit total pressure

θ_{cr} squared ratio of critical velocity at turbine inlet to critical velocity at U.S. standard atmospheric temperature, $\left[(V_{cr,0})/(1019.46)\right]^2$

ν blade-jet speed ratio, $U_3/\sqrt{2gJ\ \Delta h'_{id,s}}$

ρ gas density, lb/cu ft

Subscripts:

cr conditions at Mach number 1

id ideal

in incidence

R rotor

S stator

u tangential component, positive when its direction agrees with that of wheel velocity, negative when it disagrees

x meridional component, component in a plane containing axis of rotation

0 station at turbine inlet

1 station immediately upstream of stator exit

2 station where flow from stator exit is assumed to occupy entire cylindrical area

3 station immediately upstream of rotor inlet

4 station immediately downstream of rotor exit

Superscripts:

' absolute total state

" total state relative to rotor

APPENDIX B

ANALYTICAL PROCEDURE

The general method and assumptions have been indicated under METHOD OF ANALYSIS. The details of the analytical procedure are given in this section.

Stator Analysis

In the stator analysis, an iteration has been used to solve the equations. The equations will be written first, then the iteration procedure indicated. The weight-flow equation for station 0,

$$w = \rho_0 A_0 V_0$$

is written as

$$\left(\frac{\rho V}{\rho' V_{cr}}\right)_0 = \frac{w}{(\rho' A V_{cr})_0} \tag{B1}$$

For station 1, the weight-flow equation

$$w = \rho_1 A_1 V_1 \cos \alpha_1$$

is written as

$$w = \frac{p_1'}{p_0'} \left(\frac{\rho V}{\rho' V_{cr}}\right)_1 (\rho' V_{cr})_0 A_1 \cos \alpha_1 \tag{B2}$$

Since values of $(V/V_{cr})_1$ are assumed in the calculations, values of $(\rho V/\rho' V_{cr})_1$ for use in equation (B2) may be obtained from the identity

$$\frac{\rho V}{\rho' V_{cr}} = \frac{V}{V_{cr}} \left[1 - \frac{\gamma - 1}{\gamma + 1} \left(\frac{V}{V_{cr}}\right)^2\right]^{\frac{1}{\gamma - 1}} \tag{B3}$$

Solutions of this equation are tabulated in reference 7 and are convenient for hand calculations. The pressure ratio p_1'/p_0' is given by the equation

$$\frac{p_1'}{p_0'} = \left\{ 1 - \frac{\frac{\gamma - 1}{\gamma + 1} K_1 \left[\left(\frac{V}{V_{cr}} \right)_0^2 + \left(\frac{V}{V_{cr}} \right)_1^2 \right]}{1 - \frac{\gamma - 1}{\gamma + 1} \left(\frac{V}{V_{cr}} \right)_1^2} \right\}^{\frac{\gamma}{\gamma - 1}} \tag{B4}$$

This equation has been derived by using the assumption that the viscous loss between station 0 and station 1 is given by

$$L_1 = K_1 \frac{V_0^2 + V_1^2}{2gJ} \tag{B5}$$

The method used to evaluate K_1 is described in appendix C.

The iteration for solving equations (B1) to (B4) is as follows:

(1) For a particular value of $(V/V_{cr})_1$, assume a value of p_1'/p_0' near unity for use in equation (B2).

(2) Calculate a value of w from equation (B2) by using $(\rho V/\rho' V_{cr})_1$ from equation (B3) and $(\rho' V_{cr})_0$ obtained from the known inlet conditions.

(3) Use the resulting value of w in equation (B1) to obtain a value of $(\rho V/\rho' V_{cr})_0$.

(4) Use equation (B3) to get a corresponding value of $(V/V_{cr})_0$ for use in equation (B4).

(5) Solve equation (B4) for a new value of p_1'/p_0'.

(6) Using the new value of p_1'/p_0', return to step (2) and continue until the difference between successive values of p_1'/p_0' is negligible.

Stator to Rotor

In order to evaluate conditions at the rotor inlet, it is necessary first to determine conditions at station 2.

For calculating the pressure ratio p_2'/p_0', an equation similar to equation (B4) is used

$$\frac{p_2'}{p_0'} = \left\{ 1 - \frac{\frac{\gamma - 1}{\gamma + 1} K \left[\left(\frac{V}{V_{cr}} \right)_0^2 + \left(\frac{V}{V_{cr}} \right)_2^2 \right]}{1 - \frac{\gamma - 1}{\gamma + 1} \left(\frac{V}{V_{cr}} \right)_2^2} \right\}^{\frac{\gamma}{\gamma - 1}} \tag{B6}$$

where the loss equation is

$$L_S = K \frac{V_0^2 + V_2^2}{2gJ} \tag{B7}$$

The method used to determine the coefficient K is described in appendix C.

Equation (B6) cannot be solved immediately for p_2'/p_0', since $(V/V_{cr})_2$ is not yet known. In order to determine this quantity, equations (B5) and (B6) are written as

$$V_{1,id}^2 - V_1^2 = K_1(V_0^2 + V_1^2)$$

$$V_{2,id}^2 - V_2^2 = K(V_0^2 + V_2^2)$$

Since it is assumed that the static pressure does not change between station 1 and station 2, then $V_{2,id}$ and $V_{1,id}$ are identical and may be eliminated from the preceding equations. The result, solved for $(V/V_{cr})_2$ is

$$\left(\frac{V}{V_{cr}} \right)_2 = \left[\frac{K_1 + 1}{K + 1} \left(\frac{V}{V_{cr}} \right)_1^2 - \frac{K - K_1}{K + 1} \left(\frac{V}{V_{cr}} \right)_0^2 \right]^{1/2} \tag{B8}$$

This result may be used in equation (B6) to obtain p_2'/p_0'.

Velocity components at station 2 will be needed, so it is necessary to determine α_2. The continuity equation between stations 1 and 2,

$$(\rho V A \cos \alpha)_1 = (\rho V A \cos \alpha)_2$$

may be written as

$$\left(\frac{\rho V}{\rho' V_{cr}} \right)_1 A_1 \cos \alpha_1 = \left(\frac{\rho V}{\rho' V_{cr}} \right)_2 \frac{p_2'}{p_1'} A_2 \cos \alpha_2$$

or

$$A_2 \cos \alpha_2 = \frac{\left(\frac{\rho V}{\rho' V_{cr}}\right)_1 A_1 \cos \alpha_1}{\left(\frac{\rho V}{\rho' V_{cr}}\right)_2 \frac{p_2'}{p_1'}} \tag{B9}$$

From the assumption that the flow direction does not change between station 1 and station 2,

$$r_2 = r_1 \frac{\sin \alpha_1}{\sin \alpha_2} \tag{B10}$$

and for $A_2 = 2\pi r_2 l$,

$$A_2 \cos \alpha_2 = 2\pi l r_1 \frac{\sin \alpha_1}{\sin \alpha_2} \cos \alpha_2$$

Solving this for $\tan \alpha_2$ gives

$$\tan \alpha_2 = \frac{2\pi r_1 l \sin \alpha_1}{A_2 \cos \alpha_2}$$

Using equation (B9) to eliminate $A_2 \cos \alpha_2$ yields

$$\tan \alpha_2 = \frac{2\pi r_1 l \left(\frac{\rho V}{\rho' V_{cr}}\right)_2 \frac{p_2'}{p_1'} \sin \alpha_1}{\left(\frac{\rho V}{\rho' V_{cr}}\right)_1 A_1 \cos \alpha_1} \tag{B11}$$

This equation and equation (B10) determine α_2 and r_2 so that all necessary quantities can now be calculated at station 2.

Velocity components can now be determined at the rotor inlet. With the assumption that conservation of angular momentum between station 2 and station 3 exists,

$$V_{u,3} r_3 = V_{u,2} r_2$$

and since $V_{cr,3} = V_{cr,2}$, $(V_u/V_{cr})_3$ may be calculated from

$$\left(\frac{V_u}{V_{cr}}\right)_3 = \frac{r_2}{r_3}\left(\frac{V}{V_{cr}}\right)_2 \sin \alpha_2 = \frac{r_1}{r_3}\left(\frac{V}{V_{cr}}\right)_2 \sin \alpha_1 \qquad \text{(B12)}$$

The continuity relation between stations 2 and 3 is $(\rho V_x A)_3 = (\rho V_x A)_2$

With the assumption of isentropic flow between stations 2 and 3, and the identity

$$\frac{\rho}{\rho'} = \left[1 - \frac{\gamma - 1}{\gamma + 1}\left(\frac{V}{V_{cr}}\right)^2\right]^{\frac{1}{\gamma-1}}$$

the continuity relation yields the velocity component

$$\left(\frac{V_x}{V_{cr}}\right)_3 = \frac{\frac{r_2}{r_3}\left(\frac{\rho V}{\rho' V_{cr}}\right)_2 \cos \alpha_2}{\left\{1 - \frac{\gamma - 1}{\gamma + 1}\left[\left(\frac{V_x}{V_{cr}}\right)_3^2 + \left(\frac{V_u}{V_{cr}}\right)_3^2\right]\right\}^{\frac{1}{\gamma-1}}} \qquad \text{(B13)}$$

This equation must be solved implicitly for $(V_x/V_{cr})_3$ using the value of $(V_u/V_{cr})_3$ calculated from equation (B12). Total pressure at station 3 is the same as that at station 2 because of the assumption of isentropic flow between these two stations.

Rotor Analysis

It will be necessary to use an iteration in order to evaluate the condition of the fluid at the rotor exit. The continuity equation between station 3 and station 4, $(\rho A W_x)_4 = (\rho A W_x)_3$ is written as

$$\left(\frac{\rho W}{\rho'' W_{cr}}\right)_4 = \left(\frac{\rho W}{\rho'' W_{cr}}\right)_3 \frac{A_3}{A_4} \frac{\cos \beta_3}{\cos \beta_4} \frac{p''_3}{p''_4} \left(\frac{T''_4}{T''_3}\right)^{1/2} \qquad \text{(B14)}$$

In this equation, A_3, A_4, and β_4 are known. The equation will be more convenient to use if the following identities are substituted:

$$\left(\frac{\rho W}{\rho'' W_{cr}}\right)_3 \cos \beta_3 = \frac{\left(\frac{\rho V_x}{\rho' V_{cr}}\right)_3}{\left(\frac{T''}{T'}\right)_3^{\frac{\gamma+1}{2(\gamma-1)}}} \tag{B15}$$

$$\frac{p''_3}{p''_4}\left(\frac{T''_4}{T''_3}\right)^{1/2} = \frac{1}{\frac{p''_4}{p''_{4,id}}\left(\frac{T''_4}{T''_3}\right)^{\frac{\gamma+1}{2(\gamma-1)}}} \tag{B16}$$

The last identity depends on

$$\frac{p''_{4,id}}{p''_3} = \left(\frac{T''_4}{T''_3}\right)^{\frac{\gamma}{\gamma-1}}$$

which, in turn, depends on $T''_4 = T''_{4,id}$, since the only change in relative total temperature is that due to radius change. With the substitution of equations (B15) and (B16), the continuity equation, equation (B14) becomes

$$\left(\frac{\rho W}{\rho'' W_{cr}}\right)_4 = \frac{\left(\frac{\rho V_x}{\rho' V_{cr}}\right)_3 \frac{A_3}{A_4 \cos \beta_4}}{\frac{p''_4}{p''_{4,id}}\left(\frac{T''}{T'}\right)_3^{\frac{\gamma+1}{2(\gamma-1)}}\left(\frac{T''_4}{T''_3}\right)^{\frac{\gamma+1}{2(\gamma-1)}}} \tag{B17}$$

In order to evaluate quantities in equation (B17), the following relations are used:

$$\left(\frac{T''}{T'}\right)_3 = 1 - \frac{\gamma - 1}{\gamma + 1}\left(\frac{2UV_u - U^2}{V_{cr}^2}\right)_3 \tag{B18}$$

$$T''_3 = T'_3\left(\frac{T''}{T'}\right)_3 \tag{B19}$$

$$\frac{T''_4}{T''_3} = 1 - \frac{U_3^2 - U_4^2}{2gJc_pT''_3} \tag{B20}$$

The only quantity in equation (B17) that cannot be evaluated at this point is $p''_4/p''_{4,id}$.

The rotor viscous losses are calculated from

$$L_R = mK \frac{W_3^2 + W_4^2}{2gJ} \tag{B21}$$

and the incidence losses are calculated from

$$L_{in} = \frac{W_3^2 \sin^2 \beta_3}{2gJ} \tag{B22}$$

These loss equations are used to derive the pressure loss ratio for the rotor in the same manner as was done for the stator:

$$\frac{p''_4}{p''_{4,id}} = \left\{ 1 - \frac{\frac{\gamma - 1}{\gamma + 1}\left[mK\left(\frac{W}{W_{cr}}\right)_4^2 + \frac{\left(\frac{W}{W_{cr}}\right)_3^2}{\frac{T''_4}{T''_3}} (mK + \sin^2 \beta_3) \right]}{1 - \frac{\gamma - 1}{\gamma + 1}\left(\frac{W}{W_{cr}}\right)_4^2} \right\}^{\frac{\gamma}{\gamma - 1}} \tag{B23}$$

The use of equations (B21) and (B22) rather than more elaborate expressions for losses may be justified on grounds of simplicity and by the fact that good overall results are obtained by their use. Evaluation of the coefficients m and K are discussed in appendix C. Quantities in equation (B23) may be evaluated as follows:

$$\left(\frac{W}{W_{cr}}\right)_3 = \frac{\left(\frac{V_x}{V_{cr}}\right)_3}{\left(\frac{T''}{T'}\right)_3^{1/2} \cos \beta_3} \tag{B24}$$

$$\cos \beta_3 = \frac{V_{x,3}}{\sqrt{V_3^2 - 2V_{u,3}U_3 + U_3^2}} \tag{B25}$$

$$\sin \beta_3 = \frac{V_{u,3} - U_3}{\sqrt{V_3^2 - 2V_{u,3}U_3 + U_3^2}} \tag{B26}$$

The iteration for obtaining values of total-pressure-loss ratio across the rotor and the leaving velocity may be performed as follows:

(1) Estimate a value of $p_4''/p_{4,id}''$ slightly smaller than unity.

(2) Calculate a value of $(\rho W/\rho'' W_{cr})_4$ using equation (B17) and obtain a corresponding value of $(W/W_{cr})_4$ from equation (B3).

(3) Use equation (B23) to calculate a new value of $p_4''/p_{4,id}''$.

(4) Return to step (2) and continue until successive values of $p_4''/p_{4,id}''$ do not differ significantly.

The overall total-pressure ratio p_4'/p_0' may be obtained from the relation

$$\frac{p_4'}{p_0'} = \frac{p_2'}{p_0'} \frac{p_4''}{p_{4,id}''} \left[\left(\frac{T''}{T'} \right)_3 \left(\frac{T_4''}{T_3''} \right) \left(\frac{T'}{T''} \right)_4 \right]^{\frac{\gamma}{\gamma - 1}} \tag{B27}$$

where all the ratios involved will have been evaluated previously except $(T'/T'')_4$, which is given by

$$\left(\frac{T'}{T''} \right)_4 = 1 + \frac{\gamma - 1}{\gamma + 1} \frac{U_4^2 + 2U_4 W_{u,4}}{W_{cr,4}^2} \tag{B28}$$

where

$$W_{cr,4} = W_{cr,3} \left(\frac{T_4''}{T_3''} \right)^{1/2} \tag{B29}$$

and

$$W_{cr,3} = \frac{\sqrt{V_3^2 - 2U_3 V_{u,3} + U_3^2}}{\left(\frac{W}{W_{cr}} \right)_3} \tag{B30}$$

The pressure ratio p_4/p_0' is required for calculating the static efficiency and may be obtained from

$$\frac{p_4}{p_0'} = \frac{p_4'}{p_0'} \frac{p_4}{p_4'} \tag{B31}$$

where

$$\frac{p_4}{p_4'} = \left[1 - \frac{\gamma - 1}{\gamma + 1} \left(\frac{V}{V_{cr}}\right)_4^2\right]^{\frac{\gamma}{\gamma-1}} \tag{B32}$$

where

$$V_4 = \left[W_4^2 \cos^2\beta_4 + (U_4 + W_4 \sin \beta_4)^2\right]^{1/2} \tag{B33}$$

and

$$V_{cr,4} = W_{cr,4}\sqrt{\left(\frac{T'}{T''}\right)_4} \tag{B34}$$

Work quantities may be calculated by momentum from vector diagram quantities as

$$\Delta h' = \frac{V_{u,3}U_3 - V_{u,4}U_4}{gJ} \tag{B35}$$

where

$$V_{u,4} = U_4 + W_4 \sin \beta_4 \tag{B36}$$

Work may also be calculated from

$$\Delta h' = c_p(T_0' - T_4') \tag{B37}$$

where

$$T_4' = \frac{T_4'}{T_4''} \frac{T_4''}{T_3''} T_3'' \tag{B38}$$

For calculating total efficiency, ideal work is obtained from

$$\Delta h'_{id,t} = c_p T_0' \left[1 - \left(\frac{p_4'}{p_0'}\right)^{\frac{\gamma-1}{\gamma}}\right] \tag{B39}$$

and for calculating static efficiency, ideal work is obtained from

$$\Delta h_{id,s} = c_p T'_0 \left[1 - \left(\frac{p_4}{p'_0} \right)^{\frac{\gamma-1}{\gamma}} \right] \tag{B40}$$

Total and static efficiencies are given by

$$\eta_t = \frac{\Delta h'}{\Delta h'_{id,t}} \tag{B41}$$

$$\eta_s = \frac{\Delta h'}{\Delta h'_{id,s}} \tag{B42}$$

APPENDIX C

DETERMINATION OF LOSS CONSTANTS

Determination of K_1

In order to evaluate the constant K_1 for use in equation (B4), the value of p_1'/p_0' was estimated at 0.972 for reference conditions using information obtained from the turbine manufacturer. The constant K_1 was obtained from equation (B4) after determining the velocity ratios at reference condition as follows. Equation (B1) gives $(\rho V/\rho' V_{cr})_0$ by using the reference value of w and determining the other quantities from inlet conditions. Equation (B3) then gives $(V/V_{cr})_0$. In a similar manner, equation (B2) gives $(\rho V/\rho' V_{cr})_1$ using the estimated value of p_1'/p_0', the reference value of w, and inlet conditions. Equation (B3) then gives $(V/V_{cr})_1$ so that K_1 may be calculated from equation (B4). The resulting value of K_1 was 0.078, which was used in the calculations.

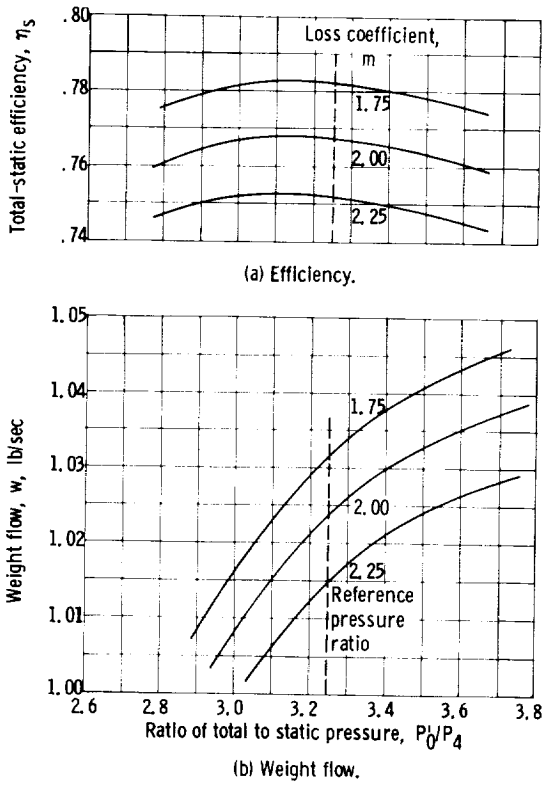

Figure 10. - Working charts for determination of m and K at 100 percent of reference speed.

Determination of K and m

The constant K was introduced in equation (B6) for the purpose of evaluating the viscous loss in the stator. Similarly, the constant m was introduced in equation (B21) to evaluate the viscous loss in the rotor. These constants were determined in such a manner that reference values of efficiency and weight flow would be calculated from the computer program at reference speed and reference pressure ratio.

The procedure used for the determination of constants K and m was as follows: Various pairs of m and K values were selected and the performance was calculated at the reference speed for each pair. From the results, for each value of K, two plots were made. One plot was efficiency against pressure ratio, and the other was weight flow against pressure ratio. Each value of m gave a separate curve on these plots. Figures 10(a) and (b) are examples of these plots for a particular value of K.

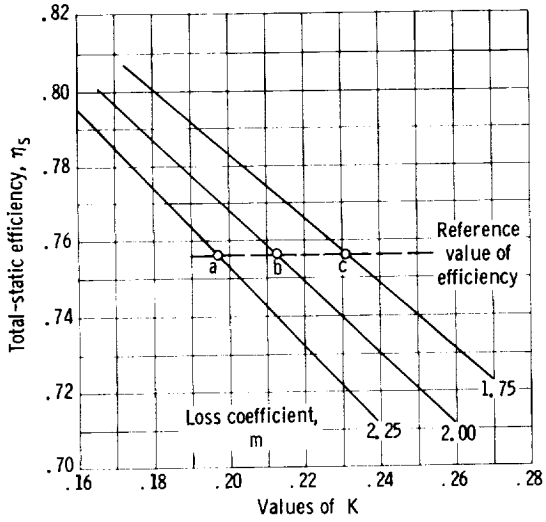

Figure 11. - Working chart for determining m and K. Constant m-lines fulfill conditions of reference speed and pressure ratio.

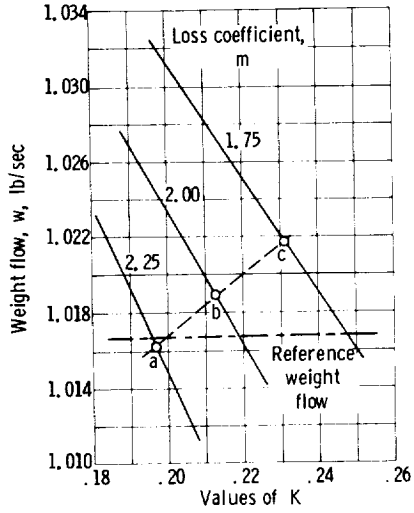

Figure 12. - Working chart for determining m and K. Constant m-lines fulfill conditions of reference speed and pressure ratio.

From a set of plots similar to figures 10(a) and (b) other plots were made by reading values of weight flow and efficiency for particular values of m and K at the reference value of pressure ratio. Figure 11 has been prepared from a set of plots similar to figure 10(a). In figure 11, the constant m curves represent points at reference pressure ratio, as well as reference speed. Similarly, figure 12 was prepared from a set of plots similar to figure 10(b), and in figure 12, the constant m curves also represent points at reference pressure ratio and reference speed.

In figure 11, points a, b, and c are points where constant m curves are intersected by a line of the reference value of efficiency. The curve through a, b, and c, then, is the locus of points, in m and K coordinates, which fulfill the conditions of reference speed, reference pressure ratio, and reference efficiency.

Transferring points a, b, and c to figure 12 permits this locus to be drawn on that figure. The point where locus a, b, and c intersects the line of reference weight flow locates the correct values of m and K. The values, for the turbine used for this report, are $m = 2.215$ and $K = 0.1995$.

REFERENCES

1. Stewart, Warner L.; Glassman, Arthur J.; and Krebs, Richard P.: The Brayton Cycle for Space Power. Paper 741A, SAE, 1963.

2. Kofskey, Milton G.; and Glassman, Arthur J.: Turbomachinery Characteristics of Brayton Cycle Space-Power Generation Systems. Paper 64-GTP-23, ASME, 1964.

3. Wood, Homer J.: Current Technology of Radial-Inflow Turbines for Compressible Fluids. Paper 62-GTP-9, ASME, 1962.

4. Whitney, Warren J.; and Stewart, Warner L.: Analytical Investigation of Performance of Two-Stage Turbine Over a Range of Ratios of Specific Heats from 1.2 to $1\frac{2}{3}$. NASA TN D-1288, 1962.

5. Wong, Robert Y.; and Nusbaum, William J.: Air-Performance Evaluation of a 4.0-Inch-Mean-Diameter Single-Stage Turbine at Various Inlet Pressures from 0.14 to 1.88 Atmospheres and Corresponding Reynolds Numbers from 2500 to 50,000. NASA TN D-1315, 1962.

6. Stewart, Warner L.; and Evans, David G.: Analytical Study of Losses at Off-Design Conditions for a Fixed-Geometry Turbine. NACA RM E53K06, 1954.

7. Whitney, Warren J.: Tabulation of Mass-Flow Parameters for Use in Design of Turbomachine Blade Rows for Ratios of Specific Heats of 1.3 and 1.4. NACA TN 3831, 1956.